JOURNAL OF MATERIALS SCIENCE **35** (2000) 1857–1866

Effect of strain rate on stepwise fatigue and creep slow crack growth in high density polyethylene

M. PARSONS, E. V. STEPANOV, A. HILTNER*, E. BAER
Department of Macromolecular Science and the Center for Applied Polymer Research, Case Western Reserve University, Cleveland, OH 44106-7202, USA
E-mail: pahle@po.cwru.edu

The effects of frequency and *R*-ratio (the ratio of minimum to maximum stress in the fatigue loading cycle) on the kinetics of step-wise crack propagation in fatigue and creep of high density polyethylene (HDPE) was characterized. Stepwise crack growth was observed over the entire range of frequency and *R*-ratio examined. A model relating crack growth rate to stress intensity factor parameters and applied strain rate was proposed by considering the total crack growth rate to consist of contributions from creep and fatigue loading components. The creep contribution in a fatigue test was calculated from the sinusoidal loading curve and the known dependence of creep crack growth on stress intensity factor in polyethylene. At a very low frequency of 0.01 Hz, fatigue crack growth rate was found to be completely controlled by creep processes. Comparison of the frequency and *R*-ratio tests revealed that the fatigue loading component depended on strain rate. Therefore, crack growth rate could be modeled with a creep contribution that depended only on the stress intensity factor parameters and a fatigue contribution that depended on strain rate.

1. Introduction

Long-term failures of structural materials often occur by slow crack growth under loads that are well below the yield stress of the material. Testing materials under exact field conditions is impractical because of the very long failure times, so prediction of long-term failure from short-term tests is desirable. Prediction of slow crack growth in polyethylene pipes used for natural gas distribution is an example where short-term testing is needed. In the field, failure occurs under mainly static loads. Elevating the test temperature is one method of accelerating failure, and a high temperature creep test (PENT test) was designed specifically for predicting long-term failure of gas-pipe resins [1]. However, the latest generation pipe resins are highly creep resistant, and the PENT test times are too long for testing the resins in a reasonable amount of time even at elevated temperature [2, 3].

Polyethylene materials retard creep crack growth by forming a tough craze in the damage zone. The craze temporarily arrests the crack until the craze fibrils deteriorate enough for the craze to rupture. As a consequence, fracture develops in a stepwise manner [4–10]. This mechanism is also inherent to failure in the field [11, 12].

Fatigue testing presents another method of accelerating fracture. A fatigue testing protocol was developed that reproduced the stepwise crack growth mechanism [4–9]. Fatigue testing was carried out at ambient temperature, which avoided possible annealing effects. The ranking of slow crack growth resistance in polyethylene pipe resins by the fatigue test followed the same ranking order as the PENT test but in up to three orders of magnitude less time [5, 6]. However, only a qualitative assessment of long-term creep failure could be made from dynamic fatigue testing.

The relationship between fatigue and creep can be quantitatively examined by systematically decreasing the dynamic component of fatigue loading. This is accomplished by varying the *R*-ratio, defined as the ratio of the minimum stress to the maximum stress in the fatigue loading cycle, so that it gradually approaches unity (creep loading). The *R*-ratio can be varied under conditions of constant maximum load or constant mean load, Fig. 1.

This approach was used to examine the relationship between fatigue and creep behavior in a high density polyethylene (HDPE) of high molecular weight [4]. Although not a modern pipe resin, the HDPE exhibited the stepwise crack propagation mechanism characteristic of field failures, and room temperature testing could be done in a reasonable amount of time even in creep loading. Stepwise crack propagation in HDPE was observed in tests under both constant maximum stress and constant mean stress loading in the tension-tension mode with *R*-ratios between 0.1 and 1.0 (creep). In this example, crack growth rate in fatigue extrapolated to the case of creep crack growth under both constant maximum and constant mean stress loading. The conservation in stepwise crack growth mechanism and

* Author to whom correspondence should be addressed.

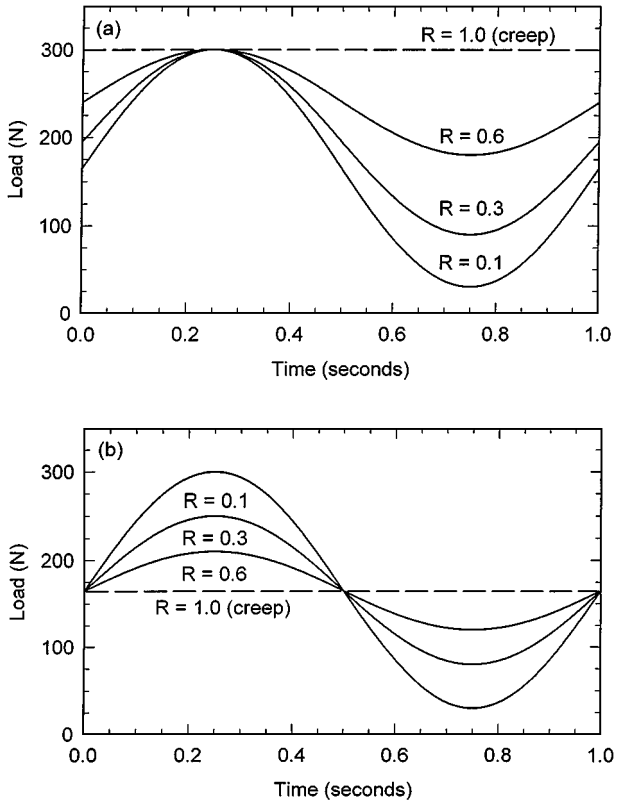

Figure 1 Fatigue loading for different R-ratios under (a) constant $K_{I,max}$ and (b) constant $K_{I,mean}$ loading.

correlation between failure kinetics in fatigue and creep tests suggested that short-term fatigue testing may be used to predict long-term creep failure properties. A power law relation in the form:

$$\frac{da}{dt} = BK_{I,max}^{4.5} K_{I,mean}^{-0.5} \tag{1}$$

where $K_{I,max}$ and $K_{I,mean}$ are the maximum and minimum stress intensity factors during the fatigue loading cycle, described crack growth rate over the entire range of fatigue and creep loading conditions.

Equation 1 reduces to the common forms of the Paris relation for slow crack growth in polyethylene, namely $da/dt \propto K_I^4$ for creep [13–15] and $da/dN \propto \Delta K_I^4$ for fatigue testing under constant R-ratio [2, 4–7, 16]. However, this relation does not take into account the effect of frequency despite the fact that in most polymers, including polyethylene, crack growth rate is frequency dependent. Furthermore, the effects of R-ratio and frequency might be interrelated because increasing R toward creep ($R = 0.1$) or decreasing frequency toward zero both have the effect of decreasing strain rate toward zero. Therefore, testing over a range of frequencies that includes very low frequencies could lead to more penetrating correlations between fatigue and creep fracture kinetics.

The effect of test frequency on fatigue crack growth rate is complex. For different polymers, the crack growth rate (expressed in units of length per number of cycles) may decrease, remain nearly constant, or increase with increasing frequency [17]. Poly(vinylchloride) (PVC) [18–21], poly(methylmethacrylate) (PMMA) [22–26], and polyethylene [16, 27, 28], for example, show a decrease in crack growth rate with increasing frequency. In one polyethylene, the number of cycles to failure was found to increase (which corresponds to a decrease in crack growth rate) in proportion to frequency raised to the 0.35 power over a range of frequencies between 0.01 and 5 Hz [27]. Crack growth rate in polycarbonate (PC) is nearly frequency independent [29, 30]. Crack growth rate in poly(vinylidene fluoride) and Nylon 6,6 increases slightly with increasing frequency [21].

Changes in crack growth rate with frequency are due to many factors: loading rate (strain rate), creep effects, and hysteretic heating are considered to be the major ones [31]. It has also been realized that if a compressive stress is part of a fatigue loading cycle (negative R-ratio), buckling of the craze fibrils is an additional frequency-sensitive mechanism of crack propagation [27]. To keep the mechanistic similarity between fatigue and creep, testing should be performed only in the tension-tension mode. Hysteretic heating can be minimized by operating at sufficiently low frequency. In polyethylene, no perceptible hysteretic heating effects were observed for frequencies at or below 1 Hz [4–9, 27, 32].

A possible way to examine strain rate and creep effects is to consider the crack growth rate to consist of superposed fatigue and creep components [31, 33] so that total crack growth rate can be expressed as:

$$\left(\frac{da}{dN}\right)_{total} = \left(\frac{da}{dN}\right)_{fatigue} + \frac{1}{f}\left(\frac{da}{dt}\right)_{creep} \tag{2}$$

where f is the fatigue frequency. It is possible to evaluate the creep component by averaging the functional dependence of the creep crack growth rate on the load over the time of the fatigue cycle. This concept successfully explained the frequency effect on crack growth rate in PMMA [26] and in Nylon 6 [33]. In Nylon 6, the contribution of the fatigue loading component decreased relative to the creep contribution with decreasing frequency and, at the lowest frequency tested of 0.1 Hz, the creep contribution was much greater than the fatigue contribution. This result suggests that, at a low enough frequency, a fatigue test might behave like a creep test, i.e. fracture is completely controlled by creep processes even though the load is cycled. However, the approach was never tested for stepwise crack propagation.

The goal of the present work was to further explore the mechanistic basis of the fatigue to creep correlation, as related to the kinetics of the stepwise crack growth, by characterizing the effect of strain rate on the deterioration of the craze damage zone. The fatigue frequency and R-ratio in the tension-tension mode were considered as the parameters that directly affected the strain rate. Variable frequency tests were performed, and evaluated together with tests with varying R-ratio. By comparing the results of these tests, the creep and fatigue contributions to crack growth rate were quantified, and a model relating crack growth rate to the fatigue loading parameters was formulated.

2. Experimental

2.1. Materials

The material used in this study was the high density polyethylene (HDPE) studied previously [4, 5]. The weight average molecular weight was 360,000 g/mol, the polydispersity ratio was 12, the density was 955 kg/m^3, and the crystallinity was 72%.

To obtain compression molded plaques about 17 mm thick, the resin was preheated at 190°C between Mylar sheets in a press; a pressure of 20 MPa was applied for 15 minutes; the pressure was rapidly cycled 10 times between 20 and 40 MPa to remove any air bubbles which could have lead to voids; and the pressure was maintained at 40 MPa for an additional 5 minutes. Plaques were cooled under pressure at a nominal rate of about 30°C/min by circulating cold water through the platens. Water circulation was maintained for an additional 30 minutes after the platens reached room temperature to ensure that the center of the plaques had cooled completely. Plaques were machined to a thickness of 13 mm. Compact tension specimens, with dimensions in compliance with ASTM D 5045-93, were cut from the plaques. Schematics illustrating the geometry and dimensions were presented previously [8]. The length, defined as the distance between the line connecting the centers of the loading pin holes and the unnotched outer edge of the specimen, was 26 mm. The height to length ratio was 1.2, and the notch length was 12.5 mm. Specimens were notched in two steps: the initial 10 mm were made by saw, and the final 2.5 mm by razor blade. The razor blade was driven into the specimen at a controlled rate of 1 μm/s. A fresh razor blade was used for each specimen.

2.2. Fatigue and creep testing under varying *R*-ratio and frequency

Mechanical fatigue units capable of applying a very stable and accurate ($\pm$0.5 N) sinusoidal load were used to conduct fatigue tests. The load and crosshead displacement were recorded by computer. A manual zoom macrolens attached to a video camera was used to observe the crack tip. The camera was routed through a VCR and video monitor and, when the test was left unattended, the experiment was recorded onto video cassette. The maximum and minimum crack tip opening displacement (CTOD), measured at the maximum and minimum stresses in the fatigue loading cycle, were taken from the video. The CTOD could only be measured for the first craze zone. In subsequent zones the top and bottom of the craze were obscured by fractured fibrils remaining from the first craze.

Fatigue tests were performed for frequencies of 1.0, 0.5, 0.2, 0.1, and 0.01 Hz under one loading condition of $K_{\mathrm{I,max}} = 1.30$ MPa(m)$^{1/2}$ and an *R*-ratio, defined as the ratio of minimum to maximum loads in the fatigue loading cycle, of 0.1. A series of tests was also run at one frequency with varying *R*-ratio between 0.1 and 1.0 (creep) under conditions of constant maximum stress and constant mean stress. Two maximum stresses, $K_{\mathrm{I,max}} = 1.30$ and 1.08 MPa(m)$^{1/2}$, were used. Under constant maximum stress, the *R*-ratio was increased by increasing the minimum stress, Fig. 1a. Two mean stresses, 0.85 and 0.72 MPa(m)$^{1/2}$, were used. Under constant mean stress, the *R*-ratio was increased by decreasing the maximum stress and increasing the minimum stress, Fig. 1b.

Fracture surfaces were examined under the light microscope to measure step jump length. Features were best resolved in bright field using normal incidence illumination. Specimens were subsequently coated with 9 nm of gold and examined in a JEOL JSM 840A scanning electron microscope. The accelerator voltage was set at 5 kV and the probe current at 6×10^{-11} amps to minimize radiation damage to the specimens.

3. Results and discussion

3.1. Effect of frequency on fatigue crack propagation

The change in crosshead displacement during fatigue testing at different frequencies is shown in Fig. 2 for $K_{\mathrm{I,max}} = 1.30$ MPa(m)$^{1/2}$ and $R = 0.1$. A test at 0.01 Hz was terminated after the second jump at about 2000 cycles. The corresponding fracture surfaces are shown in Fig. 3. Crack growth was stepwise for all the frequencies examined. The stepwise character of crack growth, which resulted from the sequential formation and fracture of a craze damage zone, was well-resolved in the plots of crosshead displacement and on the fracture surfaces. The plateaus on the plots in Fig. 2 corresponded to arrest periods during which a damage zone formed to relieve the stress concentration at the crack tip. The damage zone consisted of a main craze with a continuous membrane at the crack tip. The duration of the arrest period, which encompassed tens of thousands of cycles, corresponded to the lifetime of the damage zone. Near the end of the arrest period, the main part of the craze broke down, leaving the continuous membrane at the crack tip. The membrane then ruptured within a few thousand cycles by void formation and coalescence. A sharp increase in crosshead displacement followed membrane rupture, Fig. 2. Remnants of the broken membrane created the prominent striations on the fracture surfaces, Fig. 3.

Higher magnification SEM micrographs of two of the first craze zones in Fig. 3 are shown in Fig. 4. For all frequencies, the fracture surface consisted of

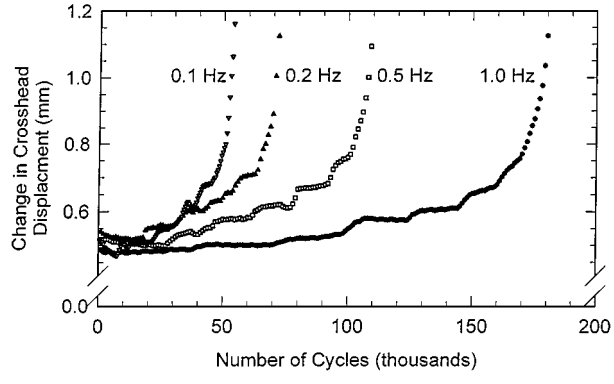

Figure 2 Crosshead displacement plotted against number of cycles for fatigue tests at frequencies of 1.0, 0.5, 0.2, and 0.1 Hz under $K_{\mathrm{I,max}} = 1.30$ MPa(m)$^{1/2}$ and $R = 0.1$.

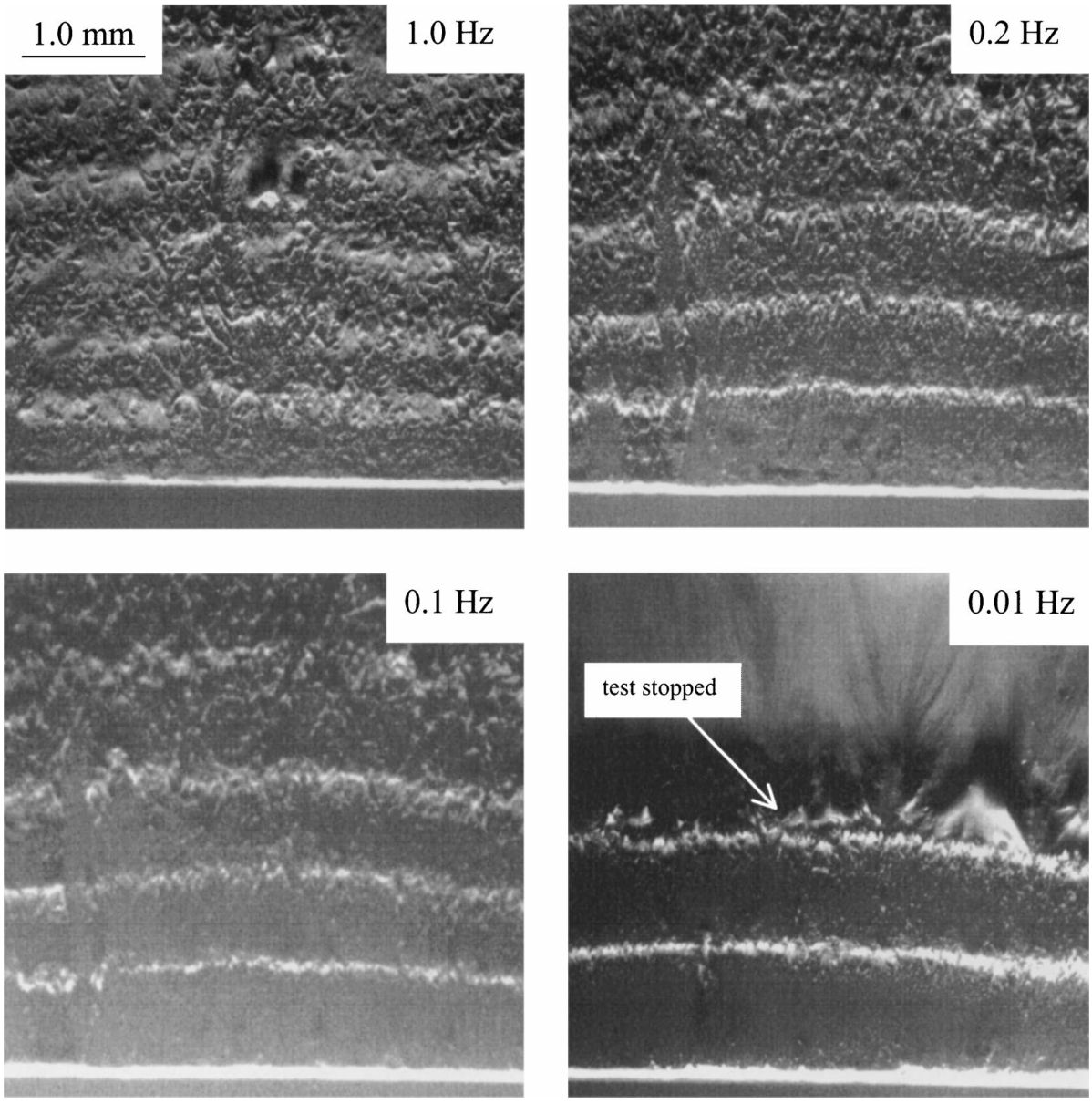

Figure 3 Fracture surfaces of specimens tested at frequencies of 1.0, 0.2, 0.1, and 0.01 Hz under $K_{I,max} = 1.30$ MPa(m)$^{1/2}$ and $R = 0.1$.

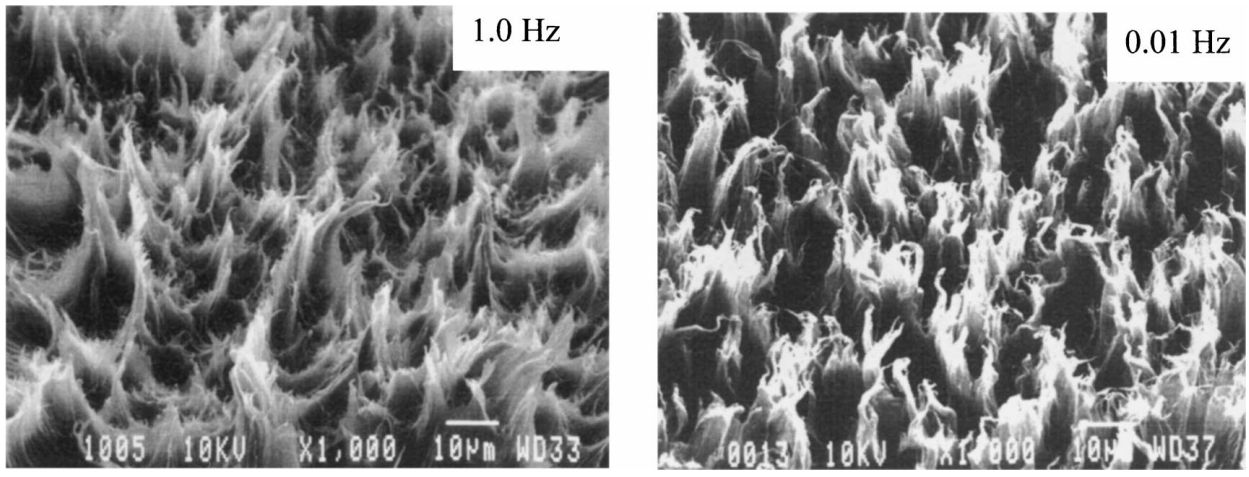

Figure 4 SEM micrographs of the first craze zone of two fracture surfaces in Fig. 3: the specimens tested at 1.0 and 0.01 Hz.

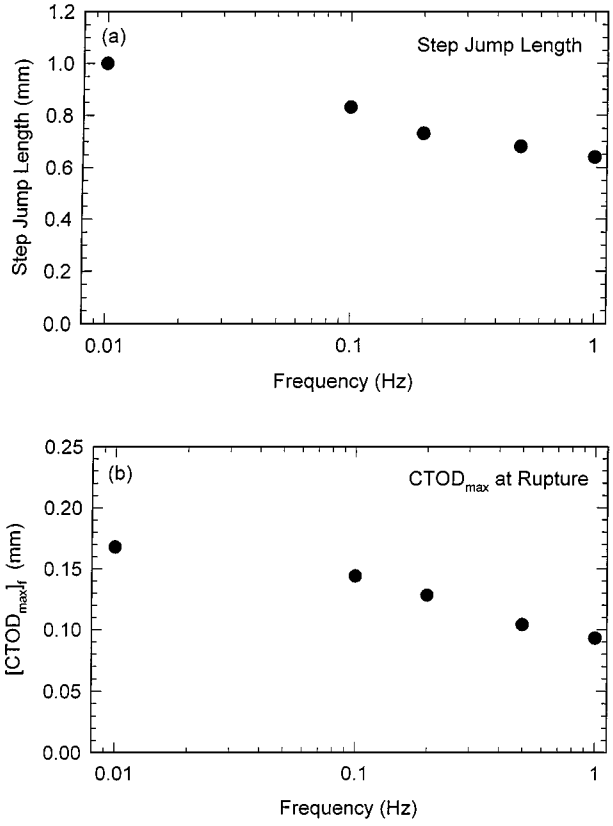

Figure 5 Effect of frequency on (a) step jump length and (b) CTOD at initiation of fracture of the first craze zone for loading under $K_{\mathrm{I,max}} = 1.30$ MPa(m)$^{1/2}$ and $R = 0.1$.

dense uniaxially drawn fibrils less than 1 μm thick. The fractography confirmed that the crack propagated by the same mechanism at all the frequencies tested and, specifically, that the crack propagated in a stepwise manner through a fibrous craze. Moreover, the crack propagation mechanism was the same as that observed previously in tests under varying R-ratio and constant frequency [4].

The crack jump length systematically increased as the frequency decreased. The length of the first jump, measured as the distance from the notch tip to the first striation on the fracture surface, increased from 0.64 to 1.00 mm as the frequency decreased from 1.0 to 0.01 Hz, Fig. 5a. Correspondingly, the crack tip opening displacement at membrane rupture $(\mathrm{CTOD})_{\mathrm{f}}$ increased from 0.09 to 0.17 mm, Fig. 5b. This was not consistent with other fatigue experiments performed at a frequency of 1 Hz with varying R-ratio [4]. In these experiments, crack jump length and $(\mathrm{CTOD})_{\mathrm{f}}$ depended only on the mean stress $K_{\mathrm{I,mean}}$, and correlated with the crack jump length and $(\mathrm{CTOD})_{\mathrm{f}}$ for creep at $K_{\mathrm{I}} = K_{\mathrm{I,mean}}$. In the 1 Hz fatigue experiments, a single loading cycle was completed in 1 sec which was negligible compared to the time scale for the craze to reach its full length. Therefore the stress that controlled the craze length was the average during the fatigue cycle, i.e. the mean stress. However, as the cycle time increased, the longer continuous exposure to the stress overshoot might have had an impact on craze growth at the microscopic level. For instance, if the cycle time approached the time scale of cavitation at $K_{\mathrm{I,max}}$, the craze could have grown beyond

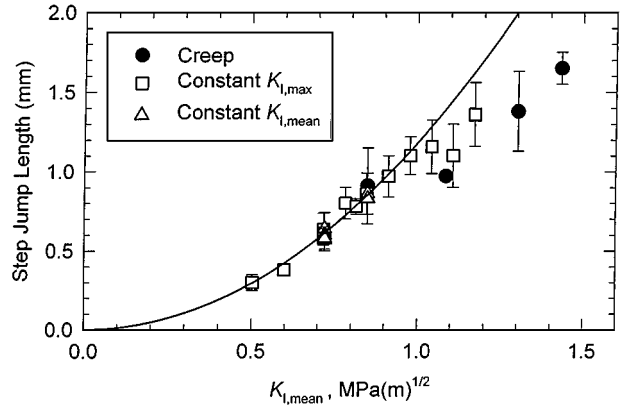

Figure 6 Effect of $K_{\mathrm{I,mean}}$ on step jump length of the first craze zone for creep tests, and for constant $K_{\mathrm{I,max}}$, and constant $K_{\mathrm{I,mean}}$ fatigue tests at 1 Hz.

the length dictated by $K_{\mathrm{I,mean}}$. Accordingly, the crack jump length for fatigue at 0.01 Hz (1.00 mm) increased to midway between that for creep at the corresponding $K_{\mathrm{I,mean}}$ (0.65 mm) and that for creep at the corresponding $K_{\mathrm{I,max}}$ (1.38 mm).

In a large number of fatigue experiments at 1 Hz and creep experiments, crack jump length and $(\mathrm{CTOD})_{\mathrm{f}}$ depended on $(K_{\mathrm{I,mean}})^2$ or $(K_{\mathrm{I}})^2$ in accordance with the Dugdale model [34, 35]. Exceptions were encountered only in tests with $K_{\mathrm{I,mean}}$ or K_{I} greater than 1.0 MPa(m)$^{1/2}$ where the damage zone length was too long for the traditional characterization in terms of the stress intensity factor to be sufficient, Fig. 6. In such a case, the gradient in K_{I} should be taken into account [8]. As a result of the general conformity of crack jump length and $(\mathrm{CTOD})_{\mathrm{f}}$ to the same dependency on $K_{\mathrm{I,mean}}$ or K_{I}, the ratio of $(\mathrm{CTOD})_{\mathrm{f}}$ to step jump length was constant and equal to 0.15 ± 0.04. This implied that the craze angle at fracture was the same even though the length and lifetime of the craze varied.

Craze growth was monitored from the crack tip opening displacement (CTOD) during the lifetime of the first craze zone. The maximum and minimum values of CTOD obtained at the maximum and minimum positions of the fatigue loading cycle, respectively, are plotted against number of cycles in Fig. 7 for a typical test ($K_{\mathrm{I,max}} = 1.30$ MPa(m)$^{1/2}$, $R = 0.1$, and $f = 1.0$ Hz).

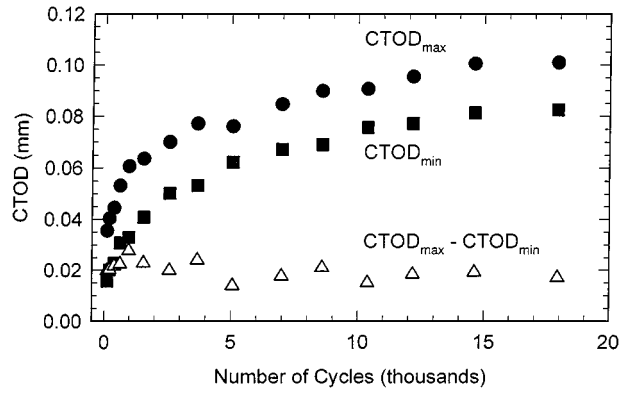

Figure 7 Growth of the maximum and minimum CTOD of the first craze zone in a typical fatigue test: $K_{\mathrm{I,max}} = 1.30$ MPa(m)$^{1/2}$, $R = 0.1$, $f = 1.0$ Hz.

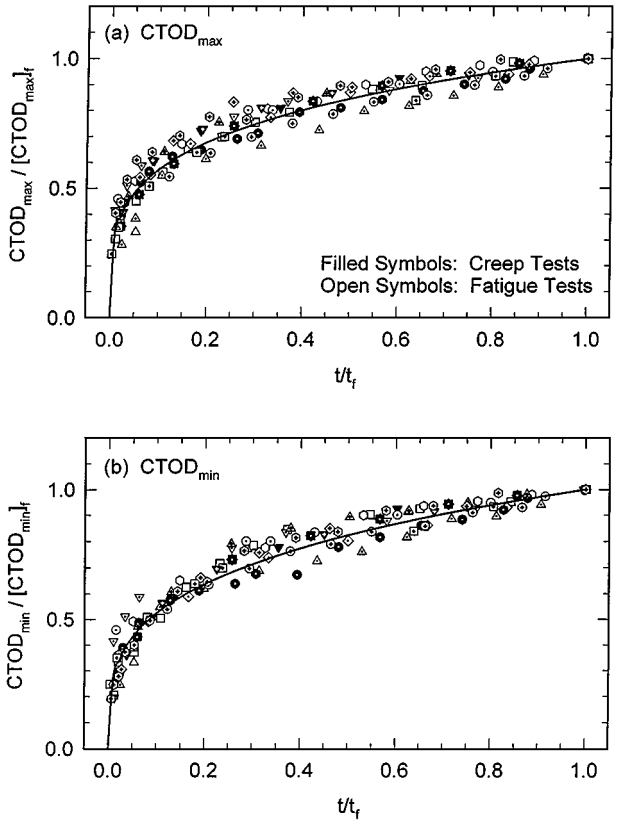

Figure 8 Relative growth rate of the (a) maximum CTOD and (b) minimum CTOD of the first craze zone for all fatigue and creep tests.

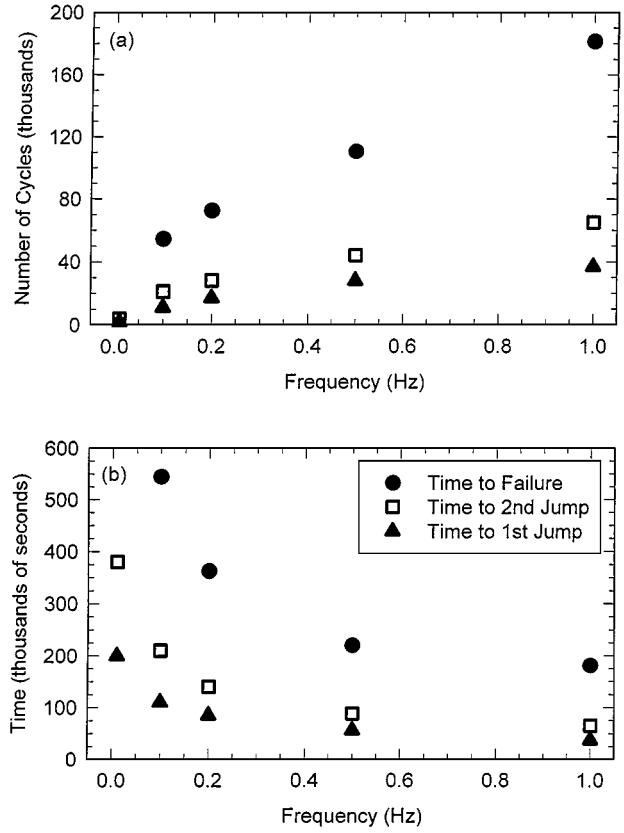

Figure 9 Effect of frequency on the duration to the first step jump, to the second step jump, and to fracture for specimens loaded under $K_{I,max} = 1.30$ MPa(m)$^{1/2}$ and $R = 0.1$. Durations are plotted as (a) number of cycles and (b) time in seconds.

Both values initially increased sharply and then gradually leveled off until the craze fractured. Despite the craze growth, the amplitude of the craze opening oscillations, $CTOD_{max} - CTOD_{min}$, remained almost constant over most of the craze lifetime.

The kinetics of craze growth was compared for all fatigue tests under different R-ratios and frequencies, including the creep experiments, by reducing $CTOD_{max}$, $CTOD_{min}$ and time t to the corresponding values at craze fracture (indicated by the subscript f). As seen in Fig. 8, the normalized data superposed within the random experimental error, which revealed a common kinetic law of the craze opening, independent of the test variables. This allowed interpolation of the normalized kinetics by a power law, $CTOD/(CTOD)_f \propto (t/t_f)^n$ where n was 0.21 ± 0.04 and 0.26 ± 0.05 for growth of the $CTOD_{max}$ and $CTOD_{min}$, respectively. The power law is usual in describing creep, and the values of n are consistent with that reported previously for polyethylene [36]. Thus, the fatigue load did not change the kinetics of craze opening. Because $(CTOD)_f$ was determined mainly by $K_{I,mean}$, the major effect of the load oscillation was on the lifetime of the damage zone t_f.

3.2. Effect of frequency and *R*-ratio on crack growth rate

Crack growth rate has been proposed as the best parameter to represent crack growth kinetics [4–7] because it relates directly to the size and lifetime of the damage zone. In stepwise crack propagation, an average crack growth rate is calculated from the length of the step jump divided by the lifetime or duration of the damage zone. The time to the first step jump (t_1), second step jump (t_{2+1}), and failure (t_f) are plotted against frequency in Fig. 9. Because of the long test time, the 0.01 Hz experiment was stopped after the second step jump. If the duration is plotted as number of cycles, Fig. 9a, t_1, t_{2+1}, and t_f decreased with decreasing frequency. If the duration is plotted as time in seconds, Fig. 9b, t_1, t_{2+1}, and t_f increased with decreasing frequency.

The corresponding crack growth rate calculated as length per cycle, da/dN, decreased with increasing frequency, Fig. 10a. The decrease in da/dN with frequency is consistent with previous observations on polyethylene [16, 27, 28] where the trend was interpreted as an improvement in fatigue crack growth resistance with increasing frequency [31]. However, this is misleading. If the crack growth rate is calculated as length per second, da/dt, the crack growth rate increased with increasing frequency, Fig. 10b. The lifetime actually decreased with increasing frequency, although the crack advanced less during each cycle. From the perspective of time, increasing frequency had a deleterious effect on the resistance to slow crack growth. Considering crack growth rate in terms of time is especially important when using fatigue as a tool for creep lifetime prediction.

The crack growth rate da/dt appeared to level off at about 0.5×10^{-5} mm/s as the frequency decreased to 0.01 Hz. The frequency-independence of da/dt at

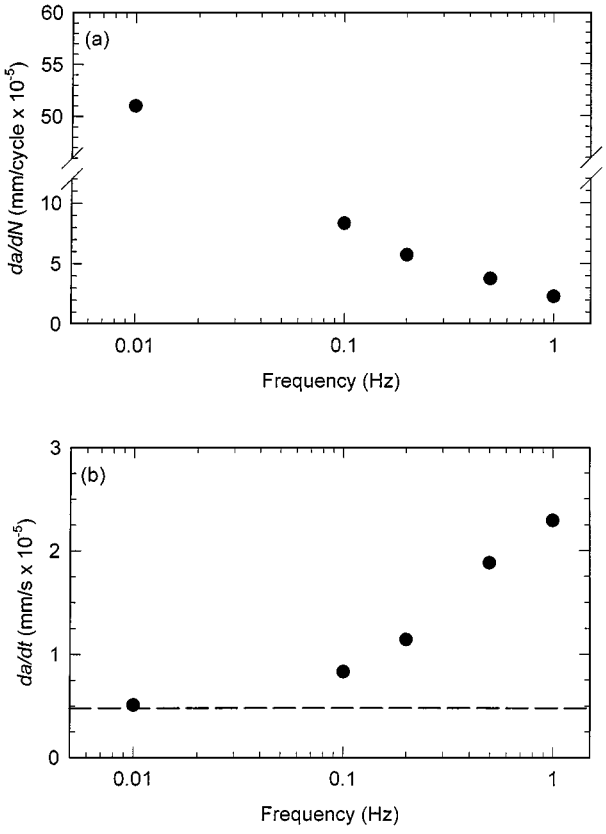

Figure 10 Effect of frequency on crack growth rate expressed as (a) mm/cycle and (b) mm/s for $K_{\mathrm{I,max}} = 1.30$ MPa(m)$^{1/2}$ and $R = 0.1$.

sufficiently low frequency indicated that extrapolation to creep, which would correspond to zero frequency, might be possible. Qualitatively, this was tested by comparing $\mathrm{d}a/\mathrm{d}t$ extrapolated from the frequency experiments with creep crack growth rates calculated from Equation 1. Equation 1 was obtained from previous experiments on the same HDPE under constant frequency, and extrapolation to creep was made by increasing the R-ratio from 0.1 to 1.0 (creep) [4]. The resulting power law relation, Equation 1, described da/dt over the entire range of loading conditions between fatigue and creep. In creep, $K_{\mathrm{I}} = K_{\mathrm{I,max}} = K_{\mathrm{I,mean}}$, and Equation 1 reduces to:

$$\frac{\mathrm{d}a}{\mathrm{d}t} = BK_{\mathrm{I}}^4 \tag{3}$$

For this HDPE, $B = 5.7 \times 10^{-6}$ mm m^2/s/MPa^4 [4]. In the experiments with varying frequency, $K_{\mathrm{I,max}}$ was 1.30 MPa(m)$^{1/2}$, and $K_{\mathrm{I,mean}}$ was 0.72 MPa(m)$^{1/2}$. Substitution of these values into Equation 3 yielded creep crack growth rates of 1.63 and 0.15×10^{-5} mm/s for $K_{\mathrm{I,max}}$ and $K_{\mathrm{I,mean}}$, respectively. The value of 0.5×10^{-5} mm/s that was obtained by extrapolating to zero frequency in Fig. 10b was intermediate between these two numbers.

The extrapolation to creep in both varying frequency and varying R-ratio experiments indicated that creep plays a major role in fatigue crack propagation. The role of creep was examined previously by considering fatigue crack growth to consist of two components [31, 33]: the crack growth due to creep and the crack growth due to true fatigue. Previously, this method was applied to continuous crack propagation, and it is not directly applicable to stepwise crack growth where the crack is arrested for much of the specimen fracture time. However, during an arrest period, craze opening due to elongation of craze fibrils is a continuous process until the craze fractures. Because drawn fibrils have practically no recovery, their creep rate under variable tensile stress should be determined by the transient magnitude of the load. On the other hand, the lifetime of the craze fibrils appeared to be inversely proportional to the rate of change in the transient load.

The creep contribution to the crack growth rate is calculated from the sinusoidal form of the loading curve and the known dependence of $\mathrm{d}a/\mathrm{d}t$ on K_{I}^4 in creep [4]. The creep contribution is expressed as:

$$\left(\frac{\mathrm{d}a}{\mathrm{d}t}\right)_{\mathrm{creep}} = B\langle K_{\mathrm{I}}^4(t)\rangle_T = \frac{B}{T}\int_T K_{\mathrm{I}}^4(t)\,\mathrm{d}t \tag{4}$$

where the integration is performed over the fatigue cycle period T. This resulted in a value of 0.48×10^{-5} mm/s for the varying frequency experiments, which was in excellent agreement with the extrapolation to zero frequency (0.5×10^{-5} mm/s). The quantity $B\langle K_{\mathrm{I}}^4(t)\rangle_T$ was calculated for all the fatigue experiments and comparison made with the measured fatigue crack growth rate. The calculated creep contribution and the measured crack growth rate for all the fatigue and creep tests are shown in Table I. In the experiments with varying R-ratio, the magnitude of either $K_{\mathrm{I,max}}$ or $K_{\mathrm{I,mean}}$ changed, so the creep contribution was different for each test. The ratio of $\mathrm{d}a/\mathrm{d}t$ and $(\mathrm{d}a/\mathrm{d}t)_{\mathrm{creep}}$ is plotted as a function of R-ratio in Fig. 11. In creep, $R = 1.0$ and the ratio is unity. As the R-ratio decreased, $\mathrm{d}a/\mathrm{d}t$ increased over the calculated $(\mathrm{d}a/\mathrm{d}t)_{\mathrm{creep}}$ and, when R was 0.1, $\mathrm{d}a/\mathrm{d}t$ was higher by a factor of 4–5. Decreasing the R-ratio increased the dynamic component of loading, and the crack growth rate accelerated due to the fatigue action.

It is important that, despite the broad range of absolute values of load that was employed in the experimental series, and the more than an order of magnitude difference in the crack growth rates, all the data

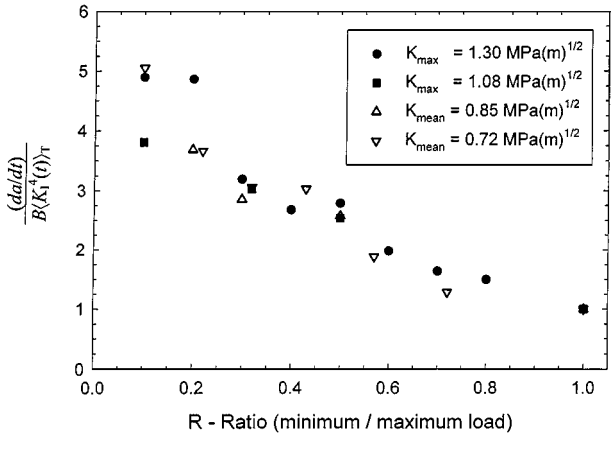

Figure 11 Effect of R-ratio on measured crack growth rate normalized to the calculated crack growth rate for creep controlled crack growth for tests at constant $K_{\mathrm{I,max}}$ and constant $K_{\mathrm{I,mean}}$ with frequency of 1 Hz.

TABLE I Effect of K_{mean}, R, and Frequency on Damage Zone Size and Crack Growth Rate

K_{mean} MPa(m)$^{1/2}$	R	Frequency Hz	Zone Lifetime s $\times 10^{-3}$	Max CTOD mm	Min CTOD mm	Jump Length mm	$(da/dt)_{creep}$ mm/s $\times 10^5$	da/dt mm/s $\times 10^5$
$K_{max} = 1.30$ MPa(m)$^{1/2}$								
0.72	0.10	1.0	26 ± 2	0.093	0.077	0.60 ± 0.10	0.48	2.29 ± 0.27
0.85	0.30	1.0	49 ± 16	0.157	0.143	0.86 ± 0.13	0.57	1.76 ± 0.67
1.04	0.60	1.0	65 ± 9	0.277	0.262	1.15 ± 0.17	0.81	1.56 ± 0.19
1.30	1.00	1.0	85 ± 20	0.349	0.349	1.38 ± 0.25	1.67	1.62 ± 0.40
$K_{max} = 1.08$ MPa(m)$^{1/2}$								
0.59	0.10	1.0	42 ± 4	0.081	0.066	0.38 ± 0.02	0.24	0.89 ± 0.09
0.72	0.32	1.0	71 ± 15	0.099	0.093	0.60 ± 0.05	0.28	0.85 ± 0.08
0.81	0.50	1.0	90 ± 16	0.121	0.114	0.78 ± 0.05	0.34	0.87 ± 0.18
1.08	1.00	1.0	120 ± 11	0.258	0.258	0.97 ± 0.02	0.81	0.81 ± 0.07
$K_{mean} = 0.85$ MPa(m)$^{1/2}$								
0.85	0.20	1.0	28 ± 3	0.131	0.111	0.84 ± 0.02	0.75	3.00 ± 0.36
0.85	0.30	1.0	49 ± 16	0.157	0.143	0.86 ± 0.13	0.57	1.76 ± 0.67
0.85	0.50	1.0	75 ± 8	0.099	0.095	0.83 ± 0.05	0.40	1.12 ± 0.25
0.85	1.00	1.0	280 ± 30	0.172	0.172	0.91 ± 0.24	0.30	0.33 ± 0.06
$K_{mean} = 0.72$ MPa(m)$^{1/2}$								
0.72	0.10	1.0	26 ± 2	0.093	0.077	0.60 ± 0.10	0.48	2.31 ± 0.27
0.72	0.32	1.0	71 ± 15	0.099	0.093	0.60 ± 0.05	0.28	0.85 ± 0.08
0.72	0.57	1.0	180 ± 50	0.099	0.096	0.57 ± 0.07	0.19	0.33 ± 0.08
0.72	1.00	1.0	435 ± 90	0.113	0.113	0.65 ± 0.07	0.15	0.15 ± 0.04
Varying Frequency								
0.72	0.10	1.00	26 ± 2	0.093	0.077	0.60 ± 0.10	0.48	2.31 ± 0.27
0.72	0.10	0.50	36 ± 5	0.104	0.082	0.68 ± 0.12	0.48	1.88 ± 0.27
0.72	0.10	0.20	64 ± 5	0.128	0.102	0.73 ± 0.12	0.48	1.14 ± 0.13
0.72	0.10	0.10	100 ± 7	0.144	0.118	0.83 ± 0.15	0.48	0.83 ± 0.10
0.72	0.10	0.01	190 ± 10	0.168	0.126	1.00 ± 0.15	0.48	0.52 ± 0.05

overlapped well enough to follow the same curve. This indicated that the fatigue acceleration in the constant frequency experiments was controlled by the R-ratio. Including also the varying frequency experiments, it is seen that all the data are described by the following equation:

$$\frac{da}{dt} = B\langle K_I^4(t)\rangle_T \beta(R, f) \tag{5}$$

where the function $\beta(R, f)$ is a fatigue acceleration factor that appears to be independent of the absolute load. As regards the parameters that affect fatigue acceleration, R-ratio determines the amplitude of the load oscillation, and f defines their time scale. Because the periodic deformation of the craze ahead of the crack tip monotonically follows the load, both parameters primarily impact the strain rate. Thus, the origin of fatigue crack growth acceleration in polyethylene should be sought in the strain rate effects.

3.3. Effect of strain rate on crack growth rate

The magnitude of the strain rate at the crack tip was defined as the average over the fatigue cycle:

$$\dot{\varepsilon} = f\left[\frac{\mathrm{CTOD_{max}} - \mathrm{CTOD_{min}}}{\mathrm{CTOD_{min}}}\right] \tag{6}$$

Except for a short initial period, the amplitude of the craze opening oscillation, $\mathrm{CTOD_{max}} - \mathrm{CTOD_{min}}$, was almost constant over the craze lifetime. In addition, $\mathrm{CTOD_{min}}$ increased rapidly early in the test and then leveled off. Although $\dot{\varepsilon}$ initially decreased, it reached a constant value for most of the test, which was taken for the strain rate evaluation.

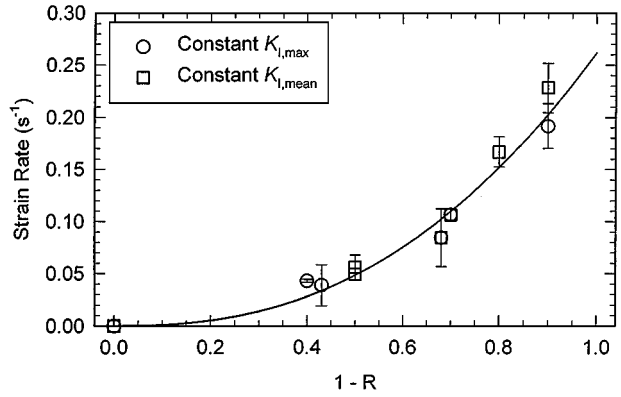

Figure 12 Relation between R-ratio and strain rate for tests at constant $K_{I,max}$ and constant $K_{I,mean}$ with frequency of 1 Hz.

The effect of R-ratio on strain rate is shown in Fig. 12 for varying R-ratio tests run under constant $K_{I,max}$ and constant $K_{I,mean}$. The data are plotted against the quantity $(1 - R) = \Delta K_I / K_{I,max}$ because the amplitudes of the strain and the stress oscillations were expected to correlate. Confirming this expectation, the strain rates for both series of tests fell on the same curve. The data were described by the relation $\dot{\varepsilon} = 0.25\,(1 - R)^2$ for $\dot{\varepsilon}$ expressed in s^{-1}.

The effect of strain rate on crack growth rate is shown in Fig. 13 where the measured crack growth rate normalized to $B\langle K_I^4(t)\rangle_T$ is plotted against strain rate for all tests with varying R-ratio and varying frequency. All the data fell on the same curve, which indicated that the acceleration in crack growth rate due to the fatigue action was dependent only on strain rate (or, specifically,

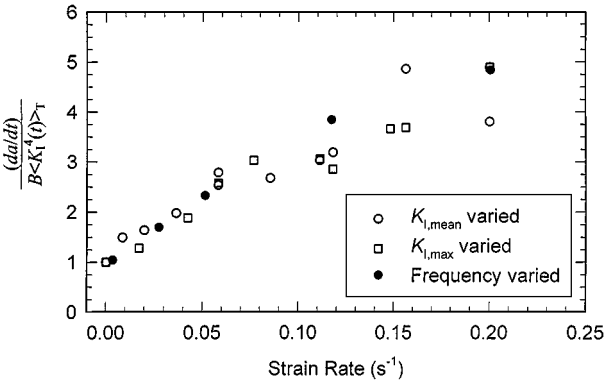

Figure 13 Effect of strain rate on measured crack growth rate normalized to the calculated crack growth rate for creep controlled crack growth in tests under varying frequency and R-ratio.

the strain and the time over which the strain was applied). Therefore, crack growth rate in fatigue can be characterized by a contribution from the creep process multiplied by a fatigue acceleration factor β that is a function of strain rate only:

$$\frac{da}{dt} = B\langle K_I^4(t)\rangle_T \beta(\dot{\varepsilon}) \qquad (7)$$

The parameter B is the same as in Equation 1. From the data in Fig. 13, an expression for β is obtained where $\beta = (1 + C\dot{\varepsilon})$ with $C = 19$ sec for strain rate given in s^{-1}.

Equation 7 takes the form of Equation 1 with an additional dependence on strain rate. The creep component of crack growth can be described by the two fatigue loading parameters $K_{I,max}$ and $K_{I,mean}$. The acceleration of crack growth due to fatigue is related to the strain rate which depends on frequency and is also affected by the fatigue loading parameters. The limitations of Equation 1, namely that the R-ratio must be greater than zero to avoid compressive damage to craze fibrils and that the crack growth mechanism must be conserved over fatigue and creep loading conditions [4], also apply to Equation 7.

Equation 7 resembles Equation 2 only in that the total crack growth rate is expressed in terms of a creep contribution and a fatigue contribution. In Equation 2 the creep and fatigue contributions are additive. By contrast, in Equation 7 the effects are multiplied. This implies that fatigue accelerates the same molecular processes as those responsible for the deterioration of the damage zone in creep. This implication is also in line with the observed similarity in the kinetics of craze opening in tension-tension mode fatigue and creep, Fig. 8. Creep in polyethylenes is usually considered as being controlled by chain disentanglement of craze fibrils [37–39]. Previous comparison of fatigue crack growth resistance of polyethylene copolymers of different molecular structure at $R = 0.1$ showed a qualitative correlation with the inferred rate of disentanglement of interlamellar tie molecules. Thus, the established mechanistic and kinetic similarities of creep and fatigue suggest that chain disentanglement concepts can be invoked as the dominant mechanism controlling the craze lifetime.

4. Conclusions

The step-wise crack growth mechanism was observed in HDPE for all the frequencies and R-ratios tested. Crack growth rate was modeled as the combined contributions from creep and fatigue loading. Calculation of the creep contribution was based on the sinusoidal loading curve and the known dependence of creep crack growth in this HDPE on K_I^4. Fatigue crack growth was completely controlled by creep processes if the frequency was low enough. Tests with different frequencies and different R-ratios were correlated by considering the strain rate at the crack tip. The fatigue component of loading was found to depend only on strain rate. The experiments confirmed a model for fatigue crack growth that consisted of a creep contribution that depended only on stress intensity factor parameters, and a fatigue contribution that depended only on strain rate.

Acknowledgement

This research was generously funded by the Gas Research Institute (contract number 5090-260-2031).

References

1. N. BROWN and X. LU, in Proceedings of the 12th Plastic Fuel Gas Pipe Symposium, Boston, MA, 1991, p. 128.
2. Y. ZHOU and N. BROWN, *Polym. Eng. Sci.* **33** (1993) 1421.
3. Y. ZHOU, X. LU and N. BROWN, *ibid.* **31** (1991) 711.
4. M. PARSONS, E. V. STEPANOV, A. HILTNER and E. BAER, *J. Mater. Sci.* **34** (1999) 3315.
5. A. SHAH, E. V. STEPANOV, G. CAPACCIO, A. HILTNER and E. BAER, *J. Polym. Sci: Part B: Polym. Phys.* **36** (1998) 2355.
6. A. SHAH, E. V. STEPANOV, M. KLEIN, A. HILTNER and E. BAER, *J. Mat. Sci.* **33** (1998) 3313.
7. A. SHAH, E. V. STEPANOV, M. KLEIN, A. HILTNER and E. BAER, in 1997 Symposium on Plastic Piping Systems for Gas Distribution, Orlando, FL, 1997, p. 235.
8. A. SHAH, E. V. STEPANOV, A. HILTNER, E. BAER and M. KLEIN, *Int. J. Fracture* **84** (1997) 159.
9. A. SHAH, E. V. STEPANOV, A. HILTNER, E. BAER and A. MOET, in SPE Conference Proceedings/54th ANTEC'96, Indianapolis, IN, 1996, Vol. 3, p. 3289.
10. X. LU, R. QIAN and N. BROWN, *J. Mater. Sci.* **26** (1991) 917.
11. K. SEHANOBISH, A. MOET, A. CHUDNOVSKY and P. P. PETRO, *J. Mater. Sci. Lett.* **4** (1985) 890.
12. A. LUSTIGER, M. J. CASSADY, F. S. URALIL and L. E. HULBERT, "Field Failure Reference Catalog for Polyethylene Gas Piping, 1st ed.," (Gas Research Institute, Chicago, 1986).
13. N. BROWN and X. LU, *Polymer* **36** (1995) 543.
14. *Idem., Int. J. Fracture* **69** (1995) 371.
15. P. A. O'CONNELL, M. J. BONNER, R. A. DUCKETT and I. M. WARD, *Polymer* **36** (1995) 2355.
16. H. NISHIMURA and I. NARISAWA, *Polym. Eng. Sci.* **31** (1991) 403.
17. R. W. HERTZBERG and J. A. MANSON, "Fatigue of Engineering Plastics," (Academic Press, New York, 1980) p. 83.
18. R. W. HERTZBERG and J. A. MANSON, *J. Mater. Sci.* **8** (1973) 1554.
19. J. C. RADON, *J. Appl. Polym. Sci.* **17** (1973) 3515.
20. J. P. ELINCK, J. C. BAUWENS and G. HOMES, *Int. J. Fracture* **7** (1971) 227.
21. R. W. HERTZBERG, J. A. MANSON and W. C. WU, *ASTM STP* **536** (1973) 391.
22. N. E. WATERS, *J. Mater. Sci.* **1** (1966) 354.
23. H. G. BORDUAS, L. E. CULVER and D. J. BURNS, *J. Strain Analysis* **3** (1968) 193.
24. N. H. WATTS and D. J. BURNS, *Polym. Eng. Sci.* **7** (1967) 90.

25. S. ARAD, J. C. RADON and L. E. CULVER, *J. Mech. Eng. Sci.* **13** (1971) 75.
26. B. MUKHERJEE and D. J. BURNS, *Experimental Mechanics* **11** (1971) 433.
27. Y. Q. ZHOU and N. BROWN, *J. Polym. Sci: Part B: Polym. Phys*. **30** (1992) 477.
28. J. A. BOWMAN, in "Buried Plastic Pipe Technology," edited by G. S. Buczala and M. J. Cassady (ASTM STP 1093: Philadelphia, 1990) p. 101.
29. J. A. MANSON and R. W. HERTZBERG, *CRC Crit. Rev. Macromol. Sci*. **1** (1973) 433.
30. R. W. HERTZBERG, M. D. SKIBO, J. A. MANSON and J. K. DONALD, *J. Mater. Sci*. **14** (1979) 1754.
31. R. W. HERTZBERG, J. A. MANSON and M. D. SKIBO, *Polym. Eng. Sci*. **15** (1975) 252.
32. J. J. STREBEL and A. MOET, *J. Polym. Sci: Part B: Polym. Phys*. **33** (1995) 1969.
33. M. G. WYZGOSKI, G. E. NOVAK and D. L. SIMON, *J. Mater. Sci*. **25** (1990) 4501.
34. D. S. DUGDALE, *J. Mech. Phys. Solids* **8** (1960) 100.
35. J. R. RICE, in "Fracture", Vol 2," edited by H. Liebowitz (Academic Press, New York, 1968) p. 191.
36. J. G. WILLIAMS and G. P. MARSHALL, *Proc. R. Soc. Lond. A* **342** (1975) 55.
37. N. BROWN and I. M. WARD, *J. Mater. Sci*. **18** (1983) 1405.
38. B. J. EGAN and O. DELATYCKI, *ibid*. **30** (1995) 3307.
39. K. FRIEDRICH, *Advances in Polymer Science* **52/53** (1983) 225.

Received 23 June
and accepted 8 September 1999